Special Feature: Spatial Information Technology towards Intelligent Vehicle Systems

Research Report

Compact Imaging LIDAR with CMOS SPAD

Hiroyuki Matsubara, Mitsuhiko Ohta, Mineki Soga, Isamu Takai and Masaru Ogawa

Report received on Feb. 8, 2018

ABSTRACT We studied a light detection and ranging (LIDAR) system to sense the surroundings of a vehicle during automated driving. We aimed to develop a small-size low-cost LIDAR with a high resolution and a long distance range. We combined a high-sensitivity light-receiving element, which is a single-photon avalanche diode (SPAD) fabricated using complementary metal-oxide-semiconductor (CMOS) technology so that the light-detection and signal-processing elements can be designed on a single chip, and a coaxial scanning optical system using a polygonal mirror, which improves the signal-to-noise ratio (SNR) by narrowing both the emitted laser beam and the light-reception field. In addition, we revised the electrical circuits to reduce the volume. The sensor has a width of 67 mm, a height of 73 mm, and a length of 177 mm. The proposed SPAD LIDAR is excellent in terms of distance performance (> 70 meters), resolution (202 × 96 pixels), cost, and robustness against optical disturbances.

KEYWORDS Lidar, Depth Sensor, Rangefinder, Single-photon Avalanche Diode, SPAD, Time-of-flight Imaging

1. Introduction

We studied a light detection and ranging (LIDAR) system for sensing the surroundings of a vehicle during automated driving. Other sensing technologies include millimeter-wave radar and cameras (including stereo cameras). Millimeter-wave radar has been used in adaptive cruise control (ACC) and pre-crash safety (PCS) systems for highways, as it can deal with a long vehicle-to-vehicle distance range, and in addition, it is robust to weather conditions (rain and fog). High-resolution cameras have been employed in lane keeping assist (LKA) and emergency braking systems (EBS) to respond to pedestrians. However, in order to implement a high level of automated driving, a sensing technology that can obtain three-dimensional (3D) information with a high spatial resolution is desired, and there have been increasing efforts to develop a corresponding LIDAR system. It is believed that LIDAR can meet the two essential requirements, long distance range and high spatial resolution. For example, when research on automated driving first began, LIDAR was used as a main sensor.[1] Even today, most experimental automated driving vehicles have LIDAR on board.

For advanced on-board LIDAR, in 2004, Ibeo presented a system with a long detection range of 200 m.[2] Thereafter, Velodyne produced a 360° high-resolution (4500 pixels horizontally and 64 vertically) LIDAR,[1] which was used in the Urban Challenge of the United States Defense Advanced Research Projects Agency (DARPA)[3] as well as in Google's experimental automated driving vehicles.[4] This system attracted significant interest as it provides important sensing technology needed for automated driving. However, the size and cost of the system are major issues for application in cars for sale to the public.

In order to overcome these challenges, extensive research on LIDAR systems has been performed. LIDAR that uses microelectromechanical-systems (MEMS) mirrors in a scanning optical system can have smaller dimensions;[5-6] however, owing to the small mirror size, they have the drawback of a limited detection distance. In addition, flash LIDAR[7] and 3D cameras,[8-9] which do not have a scanning mechanism, have also been investigated; however, as they project a wider light beam, they also have the drawback of a limited detection distance. These challenges have been mitigated by significantly strengthening the output of the light source. It is worth noting that there

is an ongoing LIDAR project (in the research stage) using an optical phased array (OPA).[10]

We aimed to realize a small-size low-cost LIDAR with a high resolution and a long distance range. We combined a single-photon avalanche diode (SPAD), which is a high-sensitivity light-receiving element, and a coaxial scanning optical system using a polygonal mirror, to realize a SPAD LIDAR that has a long distance range and high resolution.[11-13] In addition, we revised the electrical circuits to reduce the volume to one-third while maintaining the performance.[14] The proposed SPAD LIDAR was found to be excellent in terms of distance performance, cost, and robustness against optical disturbances. In this paper, we describe the proposed small-size SPAD LIDAR.

2. Overview of the SPAD LIDAR

In order to achieve a small size and a high resolution, we combined a coaxial scanning optical system and an array detector. In the coaxial scanning optical system, in addition to scanning of the emitted laser beam, the light-reception field is also scanned, and hence it is possible to improve the signal-to-noise ratio (SNR) by narrowing both the emitted laser beam and the light-reception field. The laser beam was vertically spread, and detection was performed using a linear detector array.

Figure 1 shows a schematic of the LIDAR system architecture. Pulsed light is emitted from a semiconductor laser diode (LD) with a wavelength of 905 nm, and passes through an opening in the center of a focusing parabolic mirror towards a six-facet polygonal mirror. The scattering angle of the light emitted from the LD is 1.5° (vertical) and 0.05° (horizontal). Each facet of the polygonal mirror, which rotates at a speed of 600 rpm, is set at a different tilt angle, and hence the laser light scans at six different vertical angles, providing a continuous 9° field. The scanning angle in the horizontal direction is 55° with a pitch of 0.27°; during the scan, returning light from the target is reflected from the same polygon facet and is focused by the parabolic mirror onto a complementary metal-oxide-semiconductor (CMOS) sensor chip. The light-detecting chip has 16 pixels (macropixels) arranged linearly along the vertical direction; combined with the six vertical scanning angles produced by the polygonal mirror, a vertical resolution of 96 pixels is obtained. In 1 s, 10 distance images with 202 × 96 pixels are recorded. In order to reduce background light, two types of optical filters (a visible-light cut-off filter and an interference filter), not shown in Fig. 1, are arranged in front of the sensor. **Figure 2** shows the entire LIDAR system. The sensor has a width of 67 mm, a height of 73 mm, and a length

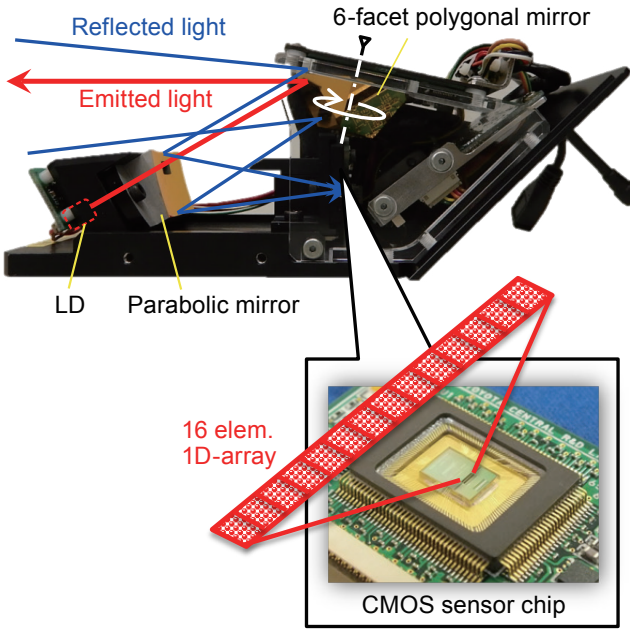

Fig. 1 Overall coaxial LIDAR architecture. A single LD is aimed coaxially at a 6-facet polygonal mirror and back-reflected photons from the targets in the scene are collected by the same facet, and are imaged onto the CMOS sensor chip at the focal plane of a parabolic mirror.

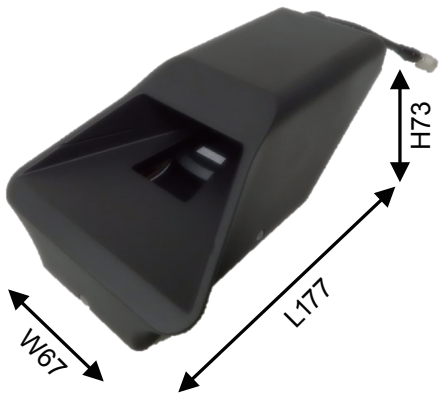

Fig. 2 Photograph of our LIDAR prototype.

of 177 mm; its specifications are provided in **Table 1**.

In order to achieve a small size, a low cost, a higher resolution, a longer-distance range, a robustness against optical disturbances, and a wide field, we developed various technologies, including a CMOS SPAD, spatiotemporal correlation, threshold control with look-ahead pixels, and rotation-axis tilting of the polygonal mirror. These technologies are described in the next section.

3. Technologies in the SPAD LIDAR

3. 1 CMOS SPAD

A SPAD is also called a Geiger-mode avalanche photodiode (APD). A reverse-bias current of at least the breakdown voltage is applied to the APD; it has an extremely high sensitivity so that it can detect even a single photon. Because the SPAD outputs an amplified digital voltage, independent of the number of detected photons, it is not possible to reveal the number of photons arriving at a given element. Therefore, in order to separate the signal light from the dark count noise and background light, which represents the noise, it is necessary to carry out measurements several times and to perform statistical processing. Thermal noise is dominant in a detector without an amplification function; however, there is no thermal noise in the SPAD, and hence reduction of the background light is the significant challenge.

We manufactured the SPAD using CMOS technology, as the light-detection and signal processing elements can be designed on a single chip; hence, a low cost is achieved. In addition, as the operating voltage is low, a high-density array can be fabricated. However, a low operating voltage implies that the width (in the thickness direction) of the region in which the signal can be converted (depletion layer) is small; therefore, the photon detection efficiency (PDE) is reduced. For short wavelengths, such as those of visible light, the Si absorption coefficient is large, and hence the absorption near the surface is relatively high and the PDE reduction is small. However, in the near-infrared region, around 900 nm, which is commonly used in current LIDAR systems, the Si absorption coefficient is small, so that photons penetrate to the back of the device, and the percentage that can be detected as a signal is reduced. We studied SPADs that can overcome these challenges by modifying the element structure.[13]

Table 1 Specification of our prototype.

Number of pixel	202 × 96
FOV	55 × 9 [degree]
Rate	10 [frames/second]
Size	W67 × H73 × L177 [mm]
Wavelength	905 [nm]
Range (at 9% reflectivity)	70 [m]

3. 2 Spatiotemporal Correlation Processing

Figure 3 shows the basic principles of the spatiotemporal correlation processing algorithm. Spatiotemporal correlation is implemented with pixels (macropixels) comprising multiple SPADs. In Fig. 3, a photon that has entered a pixel is represented by a wave-packet symbol. The black symbols (subfigure A) represent background light photons, while the red symbols (subfigure B) represent signal photons that have been reflected from the object. The signal photons

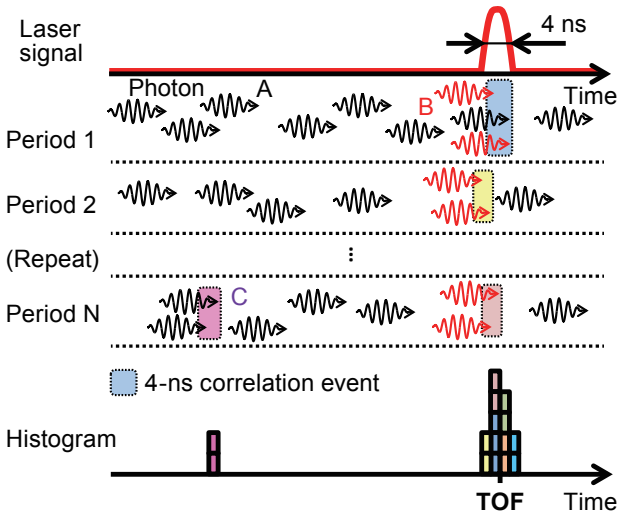

Fig. 3 Illustration of the spatiotemporal-correlated technique utilized to reject uncorrelated events such as photons from the ambient light.

are concentrated at interval widths of 4 ns (laser pulse generation), and hence they have a high correlation. On the other hand, background light photons arrive randomly in time. Only multiple photons, simultaneously detected within 4 ns, correspond to a trigger signal generated to detect the time of flight (TOF). Therefore, with this approach, it is possible to reduce the contribution of background light photons that arrive randomly in time. In addition, as the events related to the background light photons are not transmitted to the next stage of the time-to-digital converter (TDC), the effect of the TDC dead time can be significantly reduced. However, in a single measurement, even though the probability is low, it is possible for even a background light photon alone to generate an output (subfigure C). Therefore, the measurement is repeated several times (N), and the signal and background are then separated by creating histogram data.

The spatiotemporal correlation processing is implemented using the SPAD array structure shown in **Fig. 4**(a) and the circuit shown in Fig. 4(b). As shown in Fig. 4(a), one macropixel is configured from 24 SPADs. Their outputs are added in the circuit in Fig. 4(b), and threshold processing is performed. Prior to the addition, by shaping the SPAD output into the pulse from a 4-ns pulsed laser, it is possible to obtain the correct correlations within intervals of 4 ns.

3. 3 Handling Background Light with Look-ahead Pixels

We handle extremely strong background light, such as incident direct sunlight or its mirror reflection, by setting the device to first measure the amount of background light (**Fig. 5**). In the sensor chip, reference pixels are arranged alongside the TOF pixels, which are used to measure distance. The TOF pixels are arranged into arrays of 16 pixels, and they record a TOF image from the laser beam irradiation. On the other hand, the reference pixels are arranged into arrays of 32 pixels, and one time unit earlier, they measure the background light, which does not include reflected laser light. In contrast to the TOF pixels, the reference pixels do not count pulse edges, but measure the total amount of ON time. Therefore, it is possible to obtain an output that handles even extremely strong light. The reference pixels (passive intensity pixels) reveal the background light intensity, which can be employed to set threshold values in a histogram and to perform recognition processing that requires intensity information. Therefore, it is possible to perform

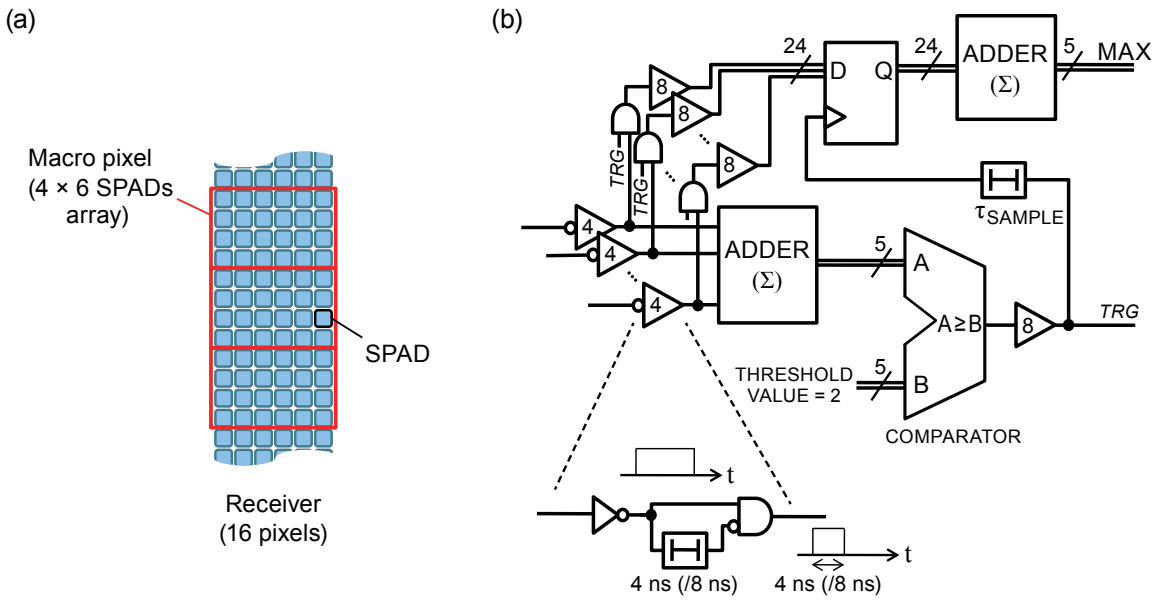

Fig. 4 Implementation of spatiotemporal-correlated photon counting technique (a) constitution of receiver (b) maximum value tracker circuit.

a distance measurement that is robust against changes in background light. The reference image has properties similar to those of intensity images recorded by cameras, and hence image recognition algorithms can be applied.

3. 4 Rotation-axis Tilting of Polygonal Mirror

By reducing the incidence and reflection angles between the light and the polygonal mirror, and by tilting the rotation axis, a relatively wide angle and undistorted field can be obtained. When scanning is performed with the polygonal mirror, the horizontal scan angle is limited by the number of polygonal facets. In the case of a six-facet polygonal mirror, the range of the rotation angle per facet that can be scanned by the emitted light beam is at most 60°. However, if the emitted light beam hits an edge of the polygonal mirror and irradiates adjacent mirrors, the signals of the reflections from the adjacent mirrors will be mixed; hence, correct data will not be obtained. Therefore, in our case, the range of rotation angle per facet is 32°. **Figure 6**(a) shows that in

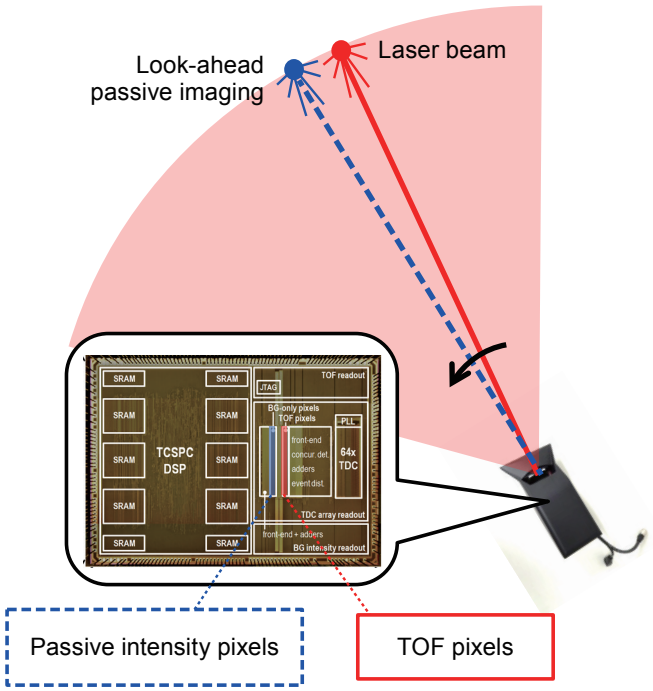

Fig. 5 Illustration of the proposed look-ahead passive imaging concept. One array of 16 pixels is utilized to measure the TOF of the active laser beam, whereas a second array of 32 pixels is utilized to perform passive imaging.

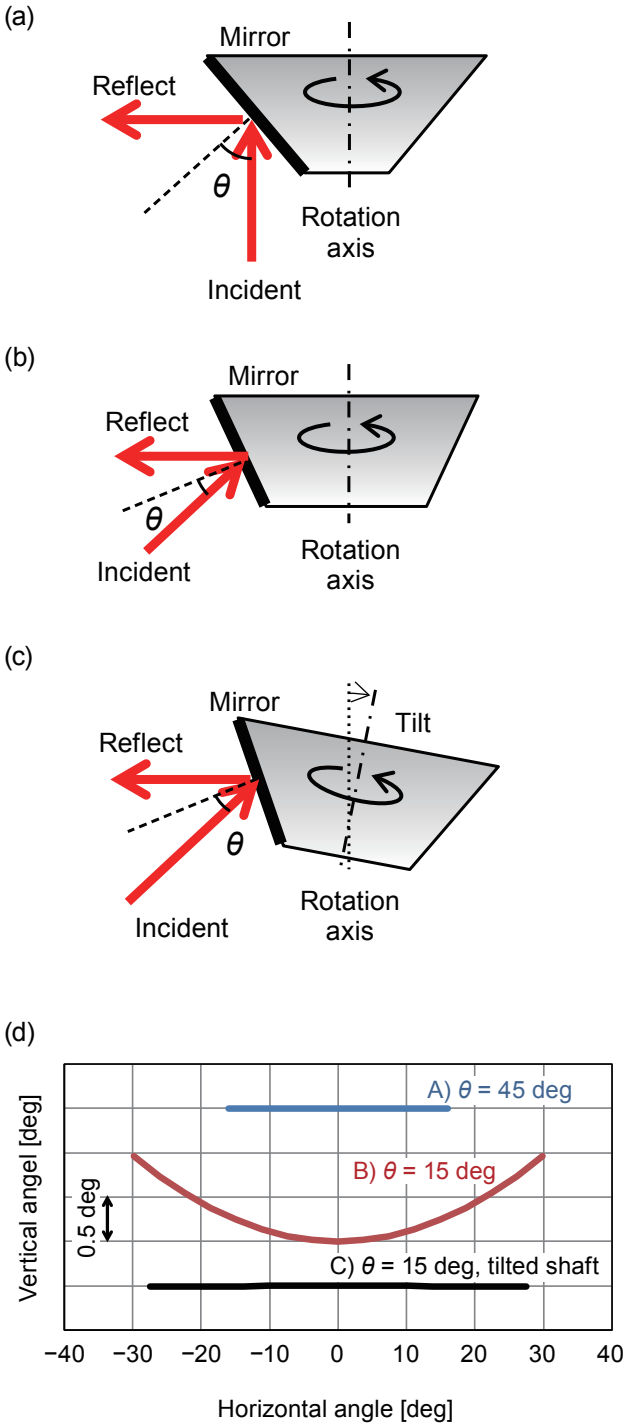

Fig. 6 Scan trajectories for scanning systems with different incidence and reflection angles θ. (a)-(c) illustration of beam and mirror, (d) scan trajectories, where the curves are offset vertically for easy viewing.

a typical arrangement, where a beam that comes directly from below is bent by 90° so as to scan horizontally, the horizontal scan range (horizontal image angle) becomes extremely narrow (32°) (Fig. 6(d), line A). On the other hand, Fig. 6(b) shows that if the incidence and reflection angles θ for the mirror are decreased, the scan angle can be widened according to the rotation angle of the mirror (Fig. 6(d), line B); however, the scan trajectory becomes distorted. In order to overcome this challenge, while the keeping incidence and reflection angles small, we tilt the rotation axis of the polygonal mirror by an appropriate angle, which causes the distortion of the scan trajectory to be reduced (Fig. 6(c)). Line C in Fig. 6(d) shows that we succeeded in maintaining a vertical angle error of less than 0.1°, while widening the horizontal scan range. Using a six-facet polygonal mirror, we can perform scanning with a horizontal image angle of 55° and with only a tiny amount of distortion.

4. Operating Examples

Next, we present several examples of measurement results with test versions of the LIDAR system. **Figure 7** shows the results of a daytime measurement in a parking lot. Figure 7(a) shows a distance image, where near distances are indicated in red and far distances are indicated in blue. Figure 7(b) shows an intensity image recorded with the look-ahead pixels; it was possible to record an image similar to that produced by an ordinary camera. Figures 7(c) and (d) show bird's-eye views, where measurement points are displayed from a viewpoint obliquely above and projected directly from above, respectively. In Figs. 7(c) and (d), the measurement points are colored according to the height; low places are indicated in red and high places are indicated in blue. This figure shows that distance data is recorded with a high resolution, and hence multiple overlapping vehicles can be separately detected.

Figure 8 shows a measurement example with backlighting. Figure 8(a) shows an image of the scene recorded with a camera. Figure 8(b) shows the LIDAR output obtained when control using the look-ahead pixels was not performed, while Fig. 8(c) shows the LIDAR output obtained when control was performed using the look-ahead pixels. Without the control using the look-ahead pixels, many incorrectly detected points appear in places other than where there are objects, while in Fig. 8(c) such incorrect detections are suppressed, and it is possible to clearly detect the front car and objects in the road environment such as posts.

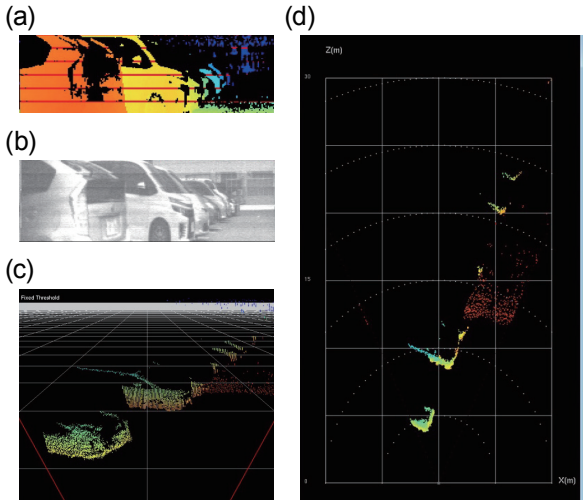

Fig. 7 Measurement result of our LIDAR (a) depth map (b) passive image (c) 3D view (d) top view. In (a) the distance is color coded from red (near) to blue (far). In (c) and (d) the vertical resolution is color coded from red (bottom) to blue (top).

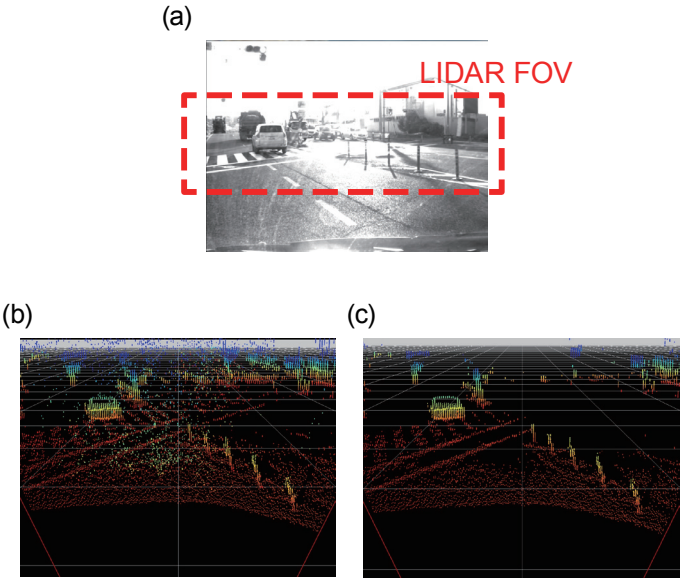

Fig. 8 Measurement result under backlight (a) camera's picture at the same time (b) 3D view of our LIDAR output without look-ahead (c) 3D view with look-ahead compensation.

5. Summary

We realized a LIDAR system for applications in vehicles, that combines a CMOS SPAD and a scanning optical system. We used a coaxial scanning optical system with a polygonal mirror, and a one-dimensional SPAD array, to realize a small-size low-cost configuration with a long distance sensitivity and a high resolution. We reduced the background light in real time using spatiotemporal correlation processing. Furthermore, we handled strong background light such as backlighting using look-ahead pixels.

Acknowledgements

The authors would like to thank C. Niclass for the great contributions he has made in our company.

Reference

(1) Glennie, C. and Lichti, D. D., "Static Calibration and Analysis of the Velodyne HDL-64E S2 for High Accuracy Mobile Scanning", *Remote Sens.*, Vol. 2, No. 6 (2010), pp. 1610-1624.
(2) Nitsche, B. and Schulz, R., "Automotive Applications for the ALASCA Laser Scanner", *Proc. Advanced Microsyst. for Automot. Appl.* (2004), pp. 119-136.
(3) Urmson, C. et al., "Autonomous Driving in Urban Environments: Boss and the Urban Challenge", *The DARPA Urban Challenge* (2009), pp. 1-59, Springer.
(4) Markoff, J., "Google Cars Drive Themselves, in Traffic", *The New York Times*, October 10, 2010, p. A1.
(5) Ito, K. et al., "System Design and Performance Characterization of a MEMS-based Laser Scanning Time-of-flight Sensor Based on a 256 × 64-pixel Single-photon Imager", *IEEE Photonics J.*, Vol. 5, No. 2 (2013), Article No. 6800114.
(6) Nippon Signal Corporation, "What's Laser Ranging Image Sensor 'Infini Soleil' ", *Nippon Signal Corporation*, <http://www.signal.co.jp/vbc/mems/sensor/>, (accessed 2017-11-30).
(7) Stettner, R., "Compact 3D flash Lidar Video Cameras and Applications", *Proc. SPIE Defense, Security, and Sensing*, Vol. 7684, No. 768405 (2010).
(8) Gokturk, B. S. et al., "A Time-Of-Flight Depth Sensor: System Description, Issues and Solutions", *Proc. Comput. Vision and Pattern Recognit. Workshop* (2004), p. 35.
(9) Niclass, C. et al., "Design and Characterization of a CMOS 3-D Image Sensor based on Single Photon Avalanche Diodes", *IEEE J. Solid-state Circuits*, Vol. 40, No. 9 (2005), pp. 1847-1854.
(10) Yaacobi, A. et al., "Integrated Phased Array for Wide-angle Beam Steering", *Opt. Lett.*, Vol. 39, No. 15 (2014), pp. 4575-4578.
(11) Niclass, C. et al., "A 100 m-Range 10-frame/s 340 × 96-Pixel Time-of-flight Depth Sensor in 0.18 μm CMOS", *IEEE J. Solid-state Circuits*, Vol. 48, No. 2 (2013), pp. 559-572.
(12) Matsubara, H. et al., "Development of Next Generation LIDAR", *R&D Review of Toyota CRDL*, Vol. 43, No. 1 (2012), pp. 7-12.
(13) Niclass, C. et al., "A 0.18 μm CMOS SoC for a 100-m-range 10-frame/s 200 × 96-pixel Time-of-flight Depth Sensor", *IEEE J. Solid-state Circuits*, Vol. 49, No. 1 (2014), pp. 315-330.
(14) Matsubara, H., "Compact Imaging LIDAR on Vehicle", *Proc. 41th Optical Symp.* (in Japanese) (2016), pp. 9-12.
(15) Takai, I. et al., "Single-photon Avalanche Diode with Enhanced NIR-sensitivity for Automotive LIDAR Systems", *Sensors*, Vol. 16, No. 4 (2016), 459.

Hiroyuki Matsubara
Research Fields:
- Optics and Optical Measurement
- LIDAR System

Academic Society:
- SPIE, the International Society for Optical Engineering

Mitsuhiko Ohta
Research Fields:
- Computer Architecture
- Research Instruments Development

Mineki Soga
Research Fields:
- Laser Range Finder
- Image Sensor for ADAS
- Computer Vision for ADAS

Isamu Takai
Research Fields:
- Single-photon Detection Systems for LIDAR
- Multifunctional Image Sensors

Academic Degree: Dr.Eng.
Academic Society:
- IEEE

Award:
- Telecom System Technology Award, the Telecommunications Advancement Foundation, 2016

Masaru Ogawa
Research Fields:
- Lidar System Design
- Signal Processing

Academic Degree: Dr.Eng.
Academic Society:
- The Institute of Electronics, Information and Communication Engineers